Signature of the nonmonotonic *d*-wave gap in electron-doped cuprates

Ilya Eremin,[1,2] Evelina Tsoncheva,[3] and Andrey V. Chubukov[3]
[1]*Max-Planck Institut für Physik Komplexer Systeme, D-01187 Dresden, Germany*
[2]*Institute für Mathematische und Theoretische Physik, TU-Braunschweig, D-38106 Braunschweig, Germany*
[3]*Department of Physics, University of Wisconsin, Madison, Wisconsin 53706, USA*
(Received 25 September 2007; published 14 January 2008)

We address the issue whether the data on optical conductivity and Raman scattering in electron-doped cuprates below T_c support the idea that the *d*-wave gap in these materials is nonmonotonic along the Fermi surface. We calculate the conductivity and Raman intensity for elastic scattering and find that a nonmonotonic gap gives rise to several specific features in optical and Raman response functions. We argue that all these features are present in the experimental data on $Nd_{2-x}Ce_xCuO_4$ and $Pr_{2-x}Ce_xCuO_4$ compounds.

DOI: 10.1103/PhysRevB.77.024508 PACS number(s): 74.72.−h, 74.25.Gz, 74.20.Mn

I. INTRODUCTION

The studies of electron-doped cuprates, $Nd_{2-x}Ce_xCuO_{4-\delta}$ (NCCO) and $Pr_{2-x}Ce_xCuO_{4-\delta}$ (PCCO), are attracting considerable attention from high-T_c community. The phase diagram of electron-doped cuprates is not as involved as in hole-doped materials. It contains sizable regions of antiferromagnetic and superconducting phases and only a small region showing pseudogap behavior.[1] The superconducting dome is centered around a quantum-critical point at which the antiferromagnetic T_N vanishes, in close similarity to phase diagrams of several heavy-fermion materials.[2]

Scanning superconducting quantum interference device,[3] angle resolved photoemission spectroscopy (ARPES),[4,5] and tunneling experiments[6] on electron-doped cuprates provided strong evidence that the gap symmetry is $d_{x^2-y^2}$, same as in hole-doped cuprates. This gap has nodes along the diagonals of the Brillouin zone and changes sign twice along the Fermi surface. The functional form of the $d_{x^2-y^2}$ gap is a more subtle issue, however. In hole-doped cuprates, the gap measured by ARPES follows reasonably well a simple *d*-wave form $\Delta(k)=\frac{\Delta_0}{2}(\cos k_x-\cos k_y)$ (equivalent to $\cos 2\phi$ for a circular Fermi surface), at least near and above optimal doping.[7] In the electron-doped cuprates, high-resolution ARPES data on the leading-edge gap in $Pr_{0.89}LaCe_{0.11}CuO_4$ (Ref. 4) show a nonmonotonic gap, with a maximum in between nodal and antinodal points on the Fermi surface. Such gap was earlier proposed in Ref. 8 as a way to explain Raman experiments in NCCO, particularly the higher frequency of the pair-breaking "2Δ" peak in the B_{2g} channel than in the B_{1g} channel. The subsequent measurements of optical conductivity $\sigma_1(\omega)$ in $Pr_{1.85}Ce_{0.15}CuO_4$ (Ref. 9) and the tunneling study between $Pr_{2-x}Ce_xCuO_4$ and lead were also interpreted as evidences of a nonmonotonic gap.[6]

The interpretation of the experimental results is still controversial, though. ARPES data on PCCO below T_c in Ref. 4 show a nonmonotonic leading-edge gap, but the spectral function all along the Fermi surface does not display a quasiparticle peak, from which one would generally infer the functional form of the gap more accurately. The interpretation of the Raman data has been criticized in Ref. 10 on the basis that, within BCS theory, the shapes of B_{1g} and B_{2g} Raman intensities for the nonmonotonic gap proposed in Ref. 8 do not agree with the data. Finally, optical results for PCCO in Ref. 9 do show a maximum at about 70 meV, which is close to $2\Delta_{max}$ inferred from B_{2g} Raman scattering. However, it is *a priori* unclear whether one should actually expect such maximum in the optical conductivity. In particular, in hole-doped materials, $\sigma_1(\omega)$ is rather smooth at $2\Delta_{max}$.[11]

From theory perspective, the nonmonotonic *d*-wave gap appears naturally under the assumption that the $d_{x^2-y^2}$ pairing is caused by the interaction with the continuum of overdamped antiferromagnetic spin fluctuations. Spin-mediated interaction is attractive in the $d_{x^2-y^2}$ channel and yields a gap which is maximal near the hot spots—the points along the Fermi surface, separated by antiferromagnetic momentum $\mathbf{Q}_{AF}$. In optimally doped NCCO and PCCO, hot spots are located close to Brillouin zone diagonals and one should generally expect the $d_{x^2-y^2}$ gap to be nonmonotonic. The self-consistent calculations within a so-called fluctuation-exchange approximation indeed demonstrated that a magnetically mediated superconducting gap shows a nonmonotonic $d_{x^2-y^2}$-wave behavior.[12,13] More specifically, the maximum of the gap is slightly shifted away from a hot spot toward the antinodal region, such that *d*-wave superconductivity with a nonmonotonic $d_{x^2-y^2}$ gap survives even when the hot spots merge at the zone diagonals.[14] In this last case, the solution of the gap equation yields

$$\Delta_\phi = \Delta_{max}\left(\frac{2\sqrt{a}}{3\sqrt{3}}\right)\frac{\cos 2\phi}{(1+a\cos^2 2\phi)^{3/2}}. \quad (1)$$

Here, ϕ is the angle along the (circular) Fermi surface ($\phi=\pi/4$ corresponds to a diagonal Fermi point), $a>1/2$ is a model-dependent parameter, and Δ_{max} is the maximum value of the gap located at $\cos 2\phi=(1/2a)^{1/2}$. The gap at various *a* is shown in Fig. 1.

As *a* increases, the nodal velocity increases, the maximum of the gap shifts toward the zone diagonal, and the value of the gap at the antinodal point $\phi=0$ decreases.

Equation (1) was successfully used in Ref. 6 to fit the superconducting gap in $Pr_{2-x}Ce_xCuO_4$ at various electron concentrations. Below, we verify whether the gap given by Eq. (1) also fits optical and Raman data. ARPES measurements[4] place the maximum of the gap slightly below

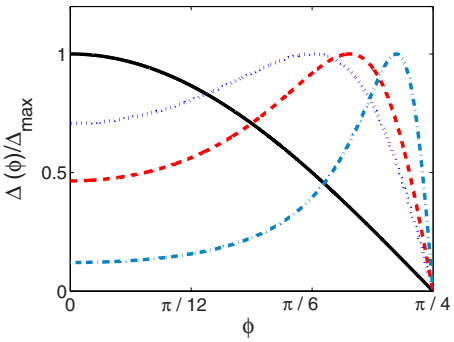

FIG. 1. (Color online) The nonmonotonic $d_{x^2-y^2}$-wave gap calculated using Eq. (1) for $a=2$ (dotted curve), $a=4$ (dashed curve), and $a=20$ (dashed-dotted curve). The black straight curve is a monotonic $d_{x^2-y^2}$-wave gap, $\Delta_\phi=\Delta_{max}\cos 2\phi$.

$\phi=\pi/6$. This is best reproduced if we set $a=2$. However, since ARPES results have not yet been confirmed by other groups, we will keep a as a parameter and present the results for different a. Note that a similar functional form of the gap can be obtained by adding higher harmonics $\cos 6\phi$, $\cos 10\phi$, etc., to the $\cos 2\phi$ gap. We found, however, that Eq. (1) is somewhat better for experimental comparisons than the gap with a few higher harmonics.

As we just said, the goal of our work is to verify to which extent optical conductivity $\sigma_1(\omega)$ and Raman scattering $R(\omega)$ in a d-wave superconductor with a gap given by Eq. (1) are consistent with the experimental data. For this, we computed $\sigma_1(\omega)$ and $R(\omega)$ in B_{1g} and B_{2g} geometries assuming that the scattering is elastic. The latter does not necessarily have to come from impurities—scattering by collective excitations in spin or charge channels is also dominated by processes with small frequency transfers. For simplicity, we assume that the normal state damping rate is independent of frequency and only focus on the effects associated with the pairing.

We have found several features which distinguish optical and Raman responses in superconductors with nonmonotonic d-wave gap from superconductors with a $\cos 2\phi$ gap. Optical conductivity in a pure d-wave superconductor with elastic scattering has a weak maximum followed by a broad suppression region at frequencies of the order Δ_{max} (Ref. 11). For the nonmonotonic gap, we have found a rather strong maximum in $\sigma_1(\omega)$ slightly below $2\Delta_{max}$, followed by a sharp drop in conductivity down to very low frequencies, where the conductivity begins to increase again toward a constant value at $\omega=0+$ (see Fig. 4). For Raman scattering, we have observed that the peak in the B_{2g} channel is located at a higher frequency than in the B_{1g} channel and also that the shapes of the two Raman profiles are very different—the B_{2g} peak is nearly symmetric and the B_{1g} peak is very asymmetric with shoulderlike behavior above the peak frequency. We argue that these features are consistent with the experimental conductivity and Raman data. From this perspective, our findings give additional support to the idea that the $d_{x^2-y^2}$ gap in electron-doped cuprates is highly nonmonotonic.

We present the formalism in Sec. II and the results in Sec. III. In the latter section, we also consider the comparison with the data in more detail. The last section is the conclusion.

II. FORMALISM

We adopt a conventional strategy of analyzing optical and Raman responses in non-s-wave superconductors with impurity scattering.[15–17] We assume that the scattering originates from the s-wave component of the effective interaction (which includes the impurity potential) and gives rise to a k-independent fermionic self-energy $\Sigma(\omega)$. The pairing comes from a different d-wave component of the interaction. As in earlier works,[15–17] we assume that the d-wave anomalous vertex is frequency independent and to a reasonable accuracy can be replaced by $\Delta(\phi)$ from Eq. (1). The time-ordered normal and anomalous fermionic Green's functions in this approximation are given by

$$G_{\mathbf{k}}(\omega,\phi)=\frac{\tilde{\omega}+\epsilon_{\mathbf{k}}}{\tilde{\omega}^2-\epsilon_{\mathbf{k}}^2-\Delta_\phi^2}, \tag{2}$$

$$F_{\mathbf{k}}(\omega,\phi)=\frac{\Delta_\phi}{\tilde{\omega}^2-\epsilon_{\mathbf{k}}^2-\Delta_\phi^2}, \tag{3}$$

where $\tilde{\omega}=\omega+\Sigma(\omega)$. The self-energy is by itself expressed via the (local) Green's function via

$$\Sigma(\omega)=i\frac{\gamma G^L(\omega)}{C^2+[G^L(\omega)]^2}, \tag{4}$$

where the local Green's function is

$$G^L(\omega)=i\frac{4}{\pi^2}\int_0^{\pi/4}\int d\epsilon_{\mathbf{k}}G_{\mathbf{k}}(\omega,\phi) \tag{5}$$

($G_L=1$ in the normal state), and the parameter C is interpolated between $C\gg 1$ in the Born limit, and $C\ll 1$ in the unitary limit. For superconductors with a monotonic gap function containing the line of nodes, the self-consistent Green's function formalism has been discussed in detail previously.[18,19]

Optical conductivity $\sigma_1(\omega)$ and Raman intensity $R(\omega)$ are both given by the combinations of bubbles made out of normal (GG) and anomalous (FF) Green's functions. Optical conductivity is proportional to the current-current correlator, while Raman intensity is proportional to the density-density correlator weighted with angle-dependent Raman vertex factors

$$\gamma_{B_{1g}}\propto\cos 2\phi,\quad \gamma_{B_{2g}}\propto\sin 2\phi. \tag{6}$$

To first approximation, B_{1g} Raman scattering then gives information about electronic states in the antinodal regions, near $\phi=0$, while B_{2g} scattering gives information about nodal regions, near $\phi=\pi/4$.

The overall sign of the FF contribution is different for $\sigma(\omega)$ and $R(\omega)$, as the running momenta in the side vertices in the FF term are $\mathbf{k}$ and $-\mathbf{k}$, between which the current operator changes sign, but the density operator remains intact. For a constant density of states, which we assume to hold, the integration over $\epsilon_{\mathbf{k}}$ in GG and FF bubbles can be performed exactly and yields

$$\sigma_1(\Omega) = -\frac{\omega_{pl}^2}{4\pi}\frac{2}{\pi\Omega}\,\mathrm{Im}\left[\int_0^{\pi/4} d\phi \int d\omega \frac{\sqrt{\tilde{\omega}_+^2-\Delta_\phi^2}\sqrt{\tilde{\omega}_-^2-\Delta_\phi^2}-\tilde{\omega}_+\tilde{\omega}_--\Delta_\phi^2}{\sqrt{\tilde{\omega}_+^2-\Delta_\phi^2}\sqrt{\tilde{\omega}_-^2-\Delta_\phi^2}\left(\sqrt{\tilde{\omega}_+^2-\Delta_\phi^2}+\sqrt{\tilde{\omega}_-^2-\Delta_\phi^2}\right)}\right], \tag{7}$$

$$R_i(\Omega) = -\frac{\sqrt{4}}{\pi^2}R_0\int_0^{\pi/4} d\phi\,\gamma_i^2\,\mathrm{Im}\left[\int d\omega \frac{\sqrt{\tilde{\omega}_+^2-\Delta_\phi^2}\sqrt{\tilde{\omega}_-^2-\Delta_\phi^2}-\tilde{\omega}_+\tilde{\omega}_-+\Delta_\phi^2}{\sqrt{\tilde{\omega}_+^2-\Delta_\phi^2}\sqrt{\tilde{\omega}_-^2-\Delta_\phi^2}\left(\sqrt{\tilde{\omega}_+^2-\Delta_\phi^2}+\sqrt{\tilde{\omega}_-^2-\Delta_\phi^2}\right)}\right]. \tag{8}$$

Here, σ_1 is the real part of the conductivity, ω_{pl} is the plasma frequency, the index i labels the various scattering geometries, $\tilde{\omega}=\omega+\Sigma(\omega)$, $\omega_\pm=\omega\pm\frac{\Omega}{2}$, and R_0 is the normalization factor for the Raman intensity. The conductivity in a superconductor also contains a $\delta(\Omega)$ contribution (not shown) related to the superconducting order parameter.

In an ideal BCS superconductor with $\tilde{\omega}=\omega$, the conductivity $\sigma_1(\omega)$ vanishes, while the Raman intensity is given by[20,21]

$$R_i(\omega) = R_0\,\mathrm{Re}\left\langle \frac{\gamma_i^2(\phi)\Delta^2(\phi)}{\omega\sqrt{\omega^2-4\Delta^2(\phi)}}\right\rangle_{FS}, \tag{9}$$

where $\langle\cdots\rangle$ denotes the averaging over the Fermi surface. For a pure d-wave gap, B_{1g} Raman intensity scales as ω^3 at small frequencies[21] and diverges logarithmically at $2\Delta_{max}$. B_{2g} intensity scales as ω at small frequencies and has a broad maximum at around $1.6\Delta_{max}$ (see Figs. 5 and 6 below).

III. RESULTS

A. Fermionic self-energy

We computed the fermionic self-energy by solving numerically the self-consistent equation [Eq. (4)] in the Born and unitary limits. The results for the imaginary part of the self-energy in the Born limit are presented in Fig. 2. For a d-wave superconductor with a monotonic gap, Im Σ is linear in frequency at small ω and has a cusp at $\omega=\Delta_{max}$. For a nonmonotonic gap, Im Σ is reduced at small frequencies and then rapidly increases to a value comparable to that for a monotonic gap. This behavior resembles, particularly for $a=2$, the formal solution of Eq. (4) for an angle-independent gap $\Delta=\Delta_{max}$. In the latter case, Im $\Sigma=0$ up to a frequency $\omega=\Delta[1-(\tilde{\gamma}/\Delta)^{2/3}]^{3/2}$, where $\tilde{\gamma}=\gamma/C^2$, and rapidly increases above this frequency. For $\tilde{\gamma}=0.05\Delta_{max}$, used in Fig. 2, the jump occurs at $\omega\approx 0.8\Delta$, much like in the plot for $a=2$. We emphasize that the solution of Eq. (4) for a constant Δ is not the result for an s-wave superconductor. For the latter, the fermionic self-energy and the pairing vertex are renormalized by the same interaction, and the self-consistent equation for $\Sigma(\omega)$ does not have the form of Eq. (4) with frequency independent Δ.

In Fig. 3, we show Im Σ in the unitary limit $C=0$. We observe the same trend. For a monotonic d-wave gap, Im Σ is nearly monotonic and has only a slight minimum around $0.8\Delta_{max}$. For a nonmonotonic gap, particularly for $a=2$, Im Σ has a more pronounced structure with a sharp minimum around $0.8\Delta_{max}$. This behavior again resembles that for a constant gap Δ. In the latter case, a formal solution of Eq. (4) for $\gamma\ll\Delta$ yields a zero Im $\Sigma(\omega)$ between $2\sqrt{\gamma\Delta}$ and $\sqrt{\Delta^2+\gamma^2}$. At larger ω, Im Σ gradually approaches the normal state value γ, and at small frequencies, it is also finite and approaches $\sqrt{\gamma\Delta}$ at zero frequency [for a generic C, a nonzero Im $\Sigma(\omega=0)$ (the unitary resonance) appears when γ exceeds $\Delta C^2\sqrt{1+C^2}$]. The region of vanishing Im Σ shrinks to zero when γ exceeds the critical value of $2\Delta/(3\sqrt{3})\approx 0.4\Delta$. For the same $\gamma=0.3\Delta_{max}$ as used in Fig. 3, Im Σ for a constant gap sharply drops around $1.1\Delta_{max}$ and rebounds both at larger and smaller frequencies, much like our actual solution for $a=2$.

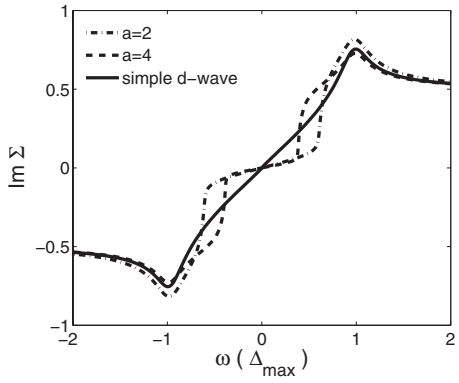

FIG. 2. The behavior of Im $\tilde{\omega}=\mathrm{Im}[\omega+\Sigma(\omega)]=\mathrm{Im}\,\Sigma(\omega)$ in the Born limit for a d-wave superconductor with a monotonic gap (solid curve) and nonmonotonic gap from Eq. (1) with $a=2$ (dashed-dotted curve) and $a=4$ (dashed curve). We used $\tilde{\gamma}=\gamma/C^2=0.05\Delta_{\max}$.

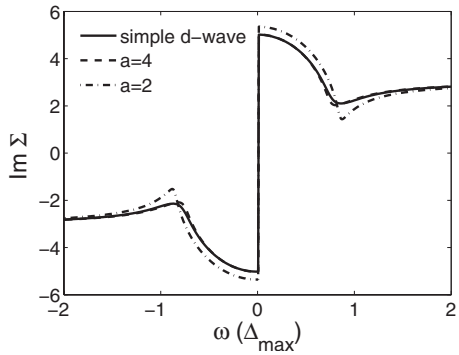

FIG. 3. The behavior of Im $\Sigma(\omega)$ in the unitary limit. Solid curve—a monotonic d-wave gap; dashed and dashed-dotted curves—a nonmonotonic gap from Eq. (1) with $a=4$ and $a=2$, respectively. We use $\gamma=0.3\Delta_{\max}$.

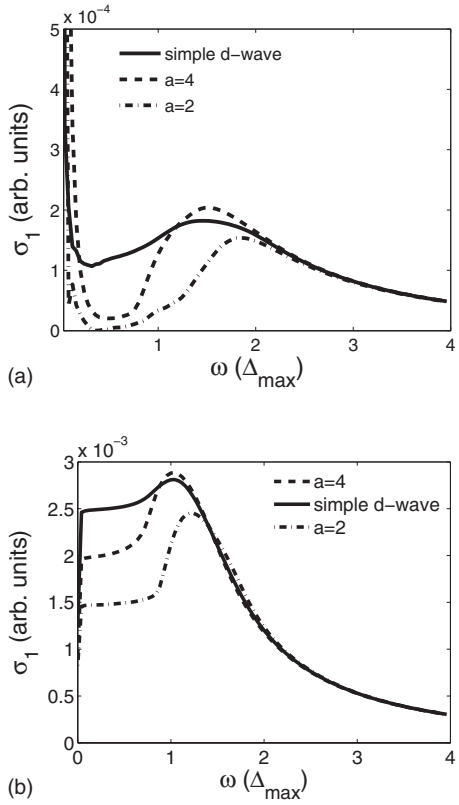

FIG. 4. The behavior of the optical conductivity $\sigma_1(\omega)$ in the (a) Born and (b) unitary limits for a monotonic gap $\Delta(\phi) \propto \cos 2\phi$ (solid line) and nonmonotonic gap with $a=2$ (dashed-dotted line) and $a=4$ (dashed line).

B. Optical conductivity

Substituting the results for the self-energy into Eq. (7), we obtain optical conductivity. The results are plotted in Figs. 4(a) and 4(b) for Born and unitary limits, respectively.[22] The behavior of the conductivity in the two limits is not identical, but the interplay between the monotonic and the nonmonotonic gap is similar. In both cases, the conductivity for a nonmonotonic gap passes through a well-pronounced maximum at some frequency below $2\Delta_{max}$, sharply drops at smaller frequencies, and then increases again at very low frequencies, and at $\omega \to 0^+$ approaches the universal limit[15] in which the conductivity depends on the nodal velocity but does not depend on γ as long as $\gamma \ll \Delta_{max}$. The universal behavior is, however, confined to very low frequencies, while in a wide frequency range below $2\Delta_{max}$, the conductivity in the case of a nonmonotonic gap is strongly reduced compared to its normal state value. The frequency at which the conductivity has a maximum depends on a and is closer to $2\Delta_{max}$ for $a=2$ than for $a=4$.

The existence of the maximum in $\sigma_1(\omega)$ below $2\Delta_{max}$ can also be understood analytically. Expanding the gap $\Delta(\phi)$ near its maximum value Δ_{max} and substituting the expansion into Eq. (7), we find, after some algebra, that the conductivity has a one-sided nonanalyticity below $\omega=2\Delta_{max}$—it contains a negative term proportional to $(2\Delta_{max}-\omega)^{3/2}$. This negative term competes with a regular part of $\sigma_1(\omega)$, which smoothly increases with decreasing ω, and gives rise to a maximum in $\sigma_1(\omega)$ below $2\Delta_{max}$.

The behavior of the conductivity in a superconductor with a nonmonotonic gap is consistent with the available data on $\sigma_1(\omega)$ in optimally doped PCCO.[9] The measured conductivity [Fig. 2(b) in Ref. 9] has a rather strong peak at 70 cm^{-1} and decreases at smaller frequencies. The authors of Ref. 9 explained the existence of the maximum in the optical conductivity by a conjecture that the conductivity in a d-wave superconductor with a nonmonotonic gap should largely resemble the conductivity in an s-wave superconductor. Our results are in full agreement with this conjecture. The authors of Ref. 9 also associated the peak frequency with $2\Delta_{max}$. We found that the peak frequency is actually located below $2\Delta_{max}$ and the difference between the two depends on the shape of the gap. For our $a=2$, the peak frequency is at $1.8\Delta_{max}$ in the Born limit and at $1.3\Delta_{max}$ in the unitary limit. For $a=4$, the deviations are higher. Experimentally, $2\Delta_{max}$ in optimally doped PCCO can be extracted from B_{2g} Raman scattering (see below) and equals 77 cm^{-1}, see Ref. 23, i.e., the peak in $\sigma_1(\omega)$ is at $1.8\Delta_{max}$. This agrees with our $a=2$ case in the Born limit.

C. Raman intensity

The results for the Raman intensity are presented in Figs. . In a BCS superconductor with a monotonic gap, Raman intensity has a sharp peak at $2\Delta_{max}$ in B_{1g} scattering geometry and a broad maximum at around $1.6\Delta_{max}$ for B_{2g} scattering. This behavior holds in the presence of impurity scattering, both in Born and unitary limits, see Figs. 5(a) and 6(a).

The B_{1g} and B_{2g} Raman intensities for a nonmonotonic gap are presented in Figs. 5(b), 5(c), 6(b), and 6(c) for Born and unitary limits and $a=2$ and $a=4$. In all cases, we find the opposite behavior: B_{2g} intensity has a sharp peak at $2\Delta_{max}$, while B_{1g} intensity is very small at small frequencies, rapidly increases around Δ_{max}, passes through a maximum, then gradually decreases at higher frequencies, and displays a weak kinklike feature at $2\Delta_{max}$. The position of the B_{1g} peak depends on a—in both Born and unitary limits, it is close to $1.6\Delta_{max}$ for $a=2$ and is close to Δ_{max} for $a=4$. Similar results have been obtained by Yoshigama and Hirashima in Ref. 13 for the inelastic scattering, the only difference is that they found B_{1g} and B_{2g} peaks located at the same frequency.

The occurrence of the 2Δ peak in B_{2g} channel at a higher frequency than in the B_{1g} channel was the main motivation in Ref. 8 to propose a nonmonotonic d-wave gap. The argument was that the gap with a maximum at intermediate $0<\phi<\pi/4$ will have more weight in the nodal region and less in the antinodal region, thus increasing the effective 2Δ for B_{2g} intensity and decreasing it for B_{1g} intensity. In the optimally doped PCCO, the B_{2g} peak occurs at 77 cm^{-1}, while the maximum in B_{1g} scattering is around 60 cm^{-1} (Fig. 2 in Ref. 23). In optimally doped NCCO, the B_{2g} peak occurs at 67 cm^{-1}, while the maximum in B_{1g} scattering is at 50 cm^{-1} (Fig. 2 in Ref. 8). The ratios of the peak positions are 1.28 in PCCO and 1.34 in NCCO. This is consistent with our result for $a=2$ (same a that gives the best fit of ARPES and con-

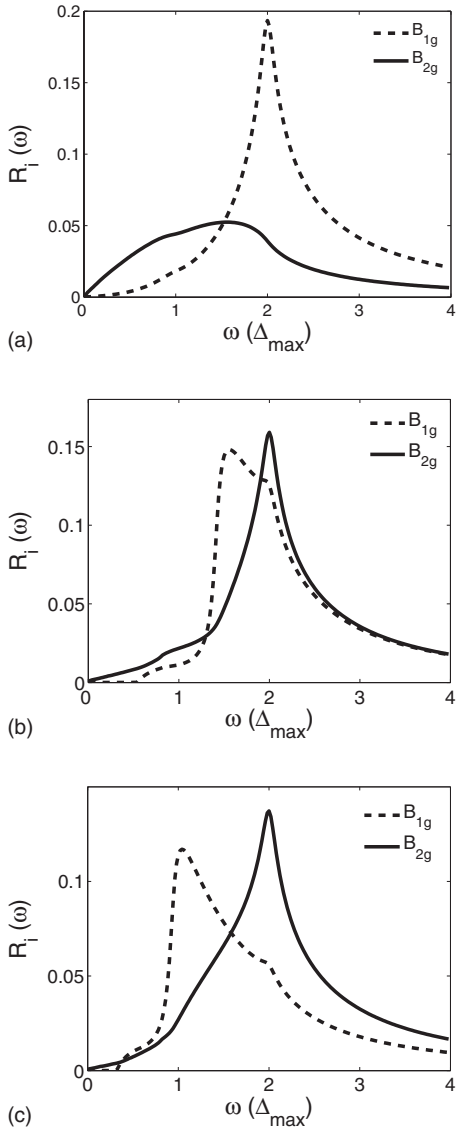

FIG. 5. The behavior of the Raman intensity $R(\omega)$ in B_{1g} (dashed) and B_{2g} (solid) scattering geometries for a monotonic gap $\Delta(\phi) \propto \cos 2\phi$ (a), and nonmonotonic gap with $a=2$ (b) and $a=4$ (c) in the Born limit.

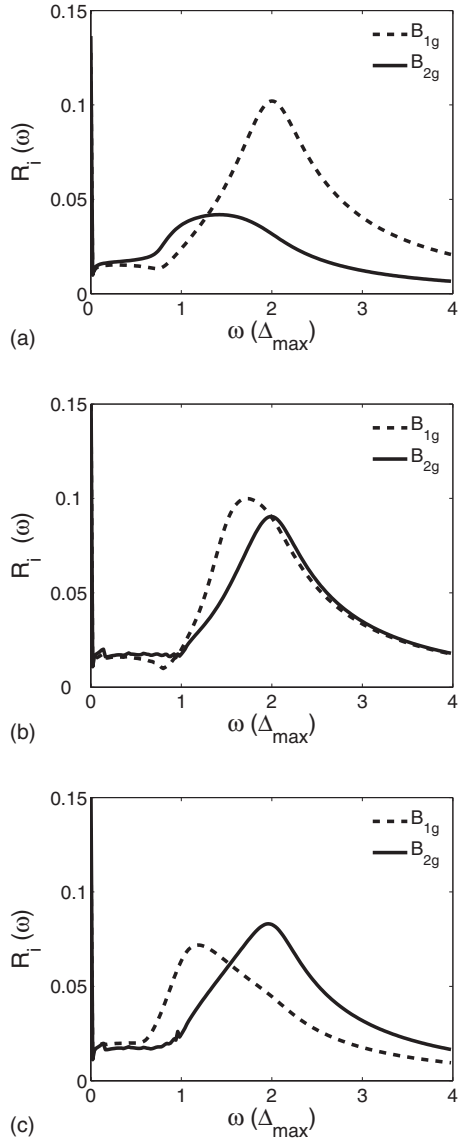

FIG. 6. The behavior of the Raman intensity $R(\omega)$ in B_{1g} (dashed) and B_{2g} (solid) scattering geometries for a monotonic gap $\Delta(\phi) \propto \cos 2\phi$ (a), and nonmonotonic gap with $a=2$ (b) and $a=4$ (c) in the unitary limit

ductivity data), for which this ratio is 1.25. Also, taking experimental 67 cm^{-1} for 2Δ in NCCO, we obtain $\Delta_{max}=4.2$ meV, in reasonable agreement with 3.7 meV observed in tunneling.[24]

In addition, the data in Fig. 3 of Ref. 8 show that the B_{2g} peak is nearly symmetric, while B_{1g} intensity is asymmetric around a maximum—it rapidly increases at frequencies around 40 cm^{-1}, passes through a maximum, and then gradually decreases at higher frequencies. This behavior of B_{1g} intensity is fully consistent with Figs. 5(b), 5(c), 6(b), and 6(c).

Blumberg *et al.*[8] also analyzed Raman intensities at various incident photon frequencies and found resonance enhancement of the B_{2g} intensity but no resonance enhancement of B_{1g} intensity. We did not attempt to analyze the resonance behavior of the Raman matrix element (this would require to consider the internal composition of the Raman vertex[26]). We note, however, that the shape of the B_{2g} Raman intensity virtually does not change between the resonance and the nonresonance cases, only the overall magnitude increases near the resonance much like it happens in resonant Raman scattering in insulating cuprates.[27] We therefore believe that our analysis of the Raman profile as a function of transferred frequency is valid both in the nonresonance and in the resonance regimes.

Finally, we note that our results for $R(\omega)$ are quite similar to Ref. 10, whose authors criticized the explanation of the Raman data in terms of nonmonotonic gap.[25] However, contrary to Ref. 10, we argue that the theoretical results for $R(\omega)$ obtained for a nonmonotonic gap agree well with the data in Ref. 8. At the same time, we agree with Ref. 10 that one can hardly extract from the data in NCCO and PCCO the ω^3 behavior of B_{1g} intensity (which is the Raman hallmark of

$d_{x^2-y^2}$ pairing), as the low-frequency behavior of the B_{1g} intensity is dominated by a sharp increase at frequencies of order Δ_{max}.

In the analysis above, we neglected the final state interaction (the renormalization of the Raman vertex). There are two reasons for this. For B_{2g} scattering, the final state interaction is given by the B_{2g} component of the effective four-fermion interaction. This component is repulsive, at least if the effective four-fermion interaction comes from spin-fluctuation exchange. The repulsive final state interaction does not give rise to excitonic resonances and generally does not substantially modify the Raman profile.[28] For B_{1g} scattering, final state interaction is the same as the pairing interaction, i.e., it is attractive. In general, such interaction affects the Raman profile.[29] However, the interaction which gives rise to a nonmonotonic gap in the form of Eq. (1) is the largest at angles ϕ close enough to $\pi/4$. At these angles, the B_{1g} matrix element $\gamma_{B_{1g}} \propto \cos 2\phi$ is reduced, and we do not expect that repeated insertions of B_{1g} vertices will substantially modify the Raman profile.

A cautionary note. Venturini *et al.*[10] argued that the nonmonotonic gap cannot explain the data on penetration depth in electron-doped materials.[30] We did not attempt to calculate the penetration depth in our formalism because it requires the knowledge of the temperature dependence of the superconducting gap function. We note, however, that a possible explanation of the penetration depth data may be provided by the conclusion drawn from tunneling experiments[6] that $Pr_{2-x}Ce_xCuO_4$ behaves as a *dirty* superconductor with a nonmonotonic gap.

IV. CONCLUSION

In this paper, we analyzed the behavior of the optical conductivity and Raman intensity in B_{1g} and B_{2g} scattering geometries in the superconducting state of electron-doped cuprates. We found that the results are best fitted by a nonmonotonic $d_{x^2-y^2}$ gap. Such gap was originally suggested as a way to explain Raman data[8] and later extracted from ARPES measurements of the leading-edge gap along the Fermi surface.[4] The nonmonotonic gap has also been obtained theoretically in the analysis of quantum-critical pairing mediated by the exchange of overdamped spin fluctuations.[12–14]

We found that the nonmonotonic gap which agrees best with the ARPES data [Eq. (1) with $a=2$] also fits best the data for optical conductivity and Raman scattering. The agreement with the data is quite good, not only in the positions of the maxima in optical conductivity and Raman response but also in the shapes of $\sigma_1(\omega)$ and $R(\omega)$. We argue that this good agreement is a strong argument in favor of a nonmonotonic $d_{x^2-y^2}$ gap in electron-doped cuprates.

ACKNOWLEDGMENTS

We thank G. Blumberg, C. Homes, and Y. Dagan for useful conversations. A.V.C. acknowledges support from Deutsche Forschungsgemeinschaft Grant No. Br118/118–1 and is thankful to TU-Braunshweig for the hospitality during the completion of this work. I.E. is supported by the DAAD under Grant No. D/05/50420.

[1] See, e.g., A. J. Millis, A. Zimmers, R. P. S. M. Lobo, N. Bontemps, and C. C. Homes, Phys. Rev. B **72**, 224517 (2005).
[2] H. v. Löhneysen, A. Rosch, M. Vojta, and P. Wölfle, Rev. Mod. Phys. **79**, 1015 (2007).
[3] C. C. Tsuei and J. R. Kirtley, Phys. Rev. Lett. **85**, 182 (2000).
[4] H. Matsui, K. Terashima, T. Sato, T. Takahashi, M. Fujita, and K. Yamada, Phys. Rev. Lett. **95**, 017003 (2005).
[5] N. P. Armitage, D. H. Lu, D. L. Feng, C. Kim, A. Damascelli, K. M. Shen, F. Ronning, Z.-X. Shen, Y. Onose, Y. Taguchi, and Y. Tokura, Phys. Rev. Lett. **86**, 1126 (2001).
[6] Y. Dagan, R. Beck, and R. L. Greene, Phys. Rev. Lett. **99**, 147004 (2007).
[7] J. C. Campuzano, M. R. Norman, and M. Randeria, in *Physics of Superconductors*, edited by K.-H. Bennemann and J. B. Ketterson (Springer, Berlin, 2004), Vol. II, pp. 167-273.
[8] G. Blumberg, A. Koitzsch, A. Gozar, B. S. Dennis, C. A. Kendziora, P. Fournier, and R. L. Greene, Phys. Rev. Lett. **88**, 107002 (2002).
[9] C. C. Homes, R. P. S. M. Lobo, P. Fournier, A. Zimmers, and R. L. Greene, Phys. Rev. B **74**, 214515 (2006).
[10] F. Venturini, R. Hackl, and U. Michelucci, Phys. Rev. Lett. **90**, 149701 (2003).
[11] D. N. Basov and T. Timusk, Rev. Mod. Phys. **77**, 721 (2005).
[12] D. Manske, I. Eremin, and K.-H. Bennemann, Phys. Rev. B **62**, 13922 (2000).
[13] H. Yoshigama and D. S. Hirashima, J. Phys. Soc. Jpn. **73**, 2057 (2004); **74**, 712 (2005).
[14] P. Krotkov and A. V. Chubukov, Phys. Rev. B **74**, 014509 (2006).
[15] P. A. Lee, Phys. Rev. Lett. **71**, 1887 (1993).
[16] See, e.g., T. Dahm, P. J. Hirschfeld, D. J. Scalapino, and L. Zhu, Phys. Rev. B **72**, 214512 (2005).
[17] A. V. Chubukov, M. R. Norman, A. J. Millis, and E. Abrahams, Phys. Rev. B **76**, 180501(R) (2007) and references therein.
[18] P. Hirshfeld, D. Vollhardt, and P. Wöllfle, Solid State Commun. **59**, 111 (1986).
[19] S. Schmitt-Rink, K. Miyake, and C. M. Varma, Phys. Rev. Lett. **57**, 2575 (1986).
[20] M. V. Klein and S. B. Dierker, Phys. Rev. B **29**, 4976 (1984).
[21] T. P. Devereaux and D. Einzel, Phys. Rev. B **51**, 16336 (1995).
[22] For the simple monotonic *d*-wave gap, our results in the unitary and Born limits agree with M. J. Graf, M. Palumbo, D. Rainer, and J. A. Sauls, Phys. Rev. B **52**, 10588 (1995).
[23] M. M. Qazilbash, A. Koitzsch, B. S. Dennis, A. Gozar, H. Balci, C. A. Kendziora, R. L. Greene, and G. Blumberg, Phys. Rev. B **72**, 214510 (2005).
[24] Q. Huang, J. F. Zasadzinski, N. Talshawala, K. E. Gray, D. G. Hinks, J. L. Peng, and R. L. Greene, Nature (London) **347**, 369 (1990).

[25] The small difference between our results and those of Ref. 10 are due to the fact that we used Eq. (1) for the gap, while they used a $\cos 2\phi$ gap with extra higher harmonics.
[26] A. V. Chubukov and D. M. Frenkel, Phys. Rev. Lett. **74**, 3057 (1995); Phys. Rev. B **52**, 9760 (1995).
[27] R. Liu, M. V. Klein, D. Salamon, S. L. Cooper, W. C. Lee, S.-W. Cheong, and D. M. Ginsberg, J. Phys. Chem. Solids **54**, 1347 (1993).
[28] H. Monien and A. Zawadowski, Phys. Rev. B **41**, 8798 (1990).
[29] A. V. Chubukov, T. P. Devereaux, and M. V. Klein, Phys. Rev. B **73**, 094512 (2006); A. Chubukov, D. Morr, and G. Blumberg, Solid State Commun. **112**, 193 (1999).
[30] J. A. Skinta, Mun-Seog Kim, T. R. Lemberger, T. Greibe, and M. Naito, Phys. Rev. Lett. **88**, 207005 (2002) and references therein.